ChemPhysChem

Research Article
doi.org/10.1002/cphc.202500012

Chemistry Europe
European Chemical Societies Publishing

www.chemphyschem.org

N-Heterocyclic Carbenes: A Benchmark Study on their Singlet–Triplet Energy Gap as a Critical Molecular Descriptor

Konstantinos P. Zois, Andreas A. Danopoulos,* and Demeter Tzeli*

N-heterocyclic carbenes (NHCs) are used extensively in modern chemistry and materials science. The in-depth understanding of their electronic structure and their metal complexes remains an important topic of research and of experimental and theoretical interest. Herein, the adiabatic singlet–triplet gap as a superior, quantifiable critical descriptor, sensitive to the nature and the structural diversity of the NHCs, for a successful rationalization of experimental observations and computationally extracted trends is established. The choice is supported by a benchmark study on the electronic structures of NHCs, using high-level *ab initio* methods, that is, complete active space self-consistent field, *n*-electron valence second-order perturbation theory, multireference configuration interaction + singles + doubles, and domain-based local pair natural orbital-coupled cluster method with single-, double-, and perturbative triple excitations along with density functional theory methods such as BP86, M06, and M06-L, B3LYP, PBE0, TPSSh, CAM-B3LYP, and B2PLYP. In contrast to the adiabatic singlet–triplet (S–T) gap preferred as descriptor, the highest occupied molecular orbital-lowest unoccupied molecular orbital gap or the S–T vertical gap that has been used in the past occasionally leads to controversial results; some of these are critically discussed below. Extrapolation of these ideas to a group of copper–NHC complexes is also described.

1. Introduction

The seminal work of Bertrand[1] and Arduengo[2] provided the experimental community with the *N*-heterocyclic carbenes (NHCs) family of molecules that enriched enormously the then arsenal of ligands. Throughout the years, NHCs have been evolved to a Swiss army knife, serving as components of transition metal catalysts[3–6] and as organocatalysts,[7,8] with many applications in polymer chemistry,[9,10] material science,[11,12] surface chemistry,[13,14] and in medicinal chemistry.

Although NHCs were initially considered as new phosphane surrogates, it soon became evident that their bonding behavior to metal centers was quite diverse. Danopoulos et al. noted that the M—C^{NHC} bonding distances in some Cu complexes were shorter than those expected for single M—C sigma bonds,[15] and Meyer et al. highlighted the involvement of other π–interactions, termed as π–backbonding.[16,17] Moreover, work by the groups of Frenking[18] and Cavallo[19] clarified these interactions by computational methods, underlining the distinctiveness of NHCs.

The early computational reports focused mainly on restricted Hartree–Fock (RHF)[20] and MPn methods, while cases using higher, multiconfigurational, methodologies have also appeared.[21–25] The advent of fast and robust density functional theory (DFT) methods has been dominating the description of the electronic structure of NHCs and complexes,[26–28] though the high-level *ab initio* methods have continuously been used, albeit less frequently.[29–38] Consequently, the mainstream of studies of NHCs that also extrapolated trends and useful heuristics[39–47] were conducted almost exclusively in terms of DFT. Importantly, a modern approach using different *ab initio* methods to benchmark the electronic structure of these molecules does not exist, to our knowledge.

In this respect, it would be desirable and welcome to assess existing critical parameters that are sensitive to the nature of the NHCs via accurate *ab initio* methods and additionally check their validity and scope also via the commonly used DFT methodology.

Generally, a plethora of metrics and descriptors has been developed for describing/evaluating the character and reactivity of NHCs:[48,49] 1) the basicity, either in Brønsted or Lewis terms, which has been studied by both experimental and computational terms;[50–53] 2) The pK_a values which feature a trend, correlating the increase in the basicity with the electron-donating properties

K. P. Zois, D. Tzeli
Laboratory of Physical Chemistry, Department of Chemistry
National and Kapodistrian University of Athens
Panepistimiopolis, 15771 Athens, Greece
E-mail: tzeli@chem.uoa.gr

K. P. Zois, A. A. Danopoulos
Laboratory of Inorganic Chemistry, Department of Chemistry
National and Kapodistrian University of Athens
Panepistimiopolis, 15771 Athens, Greece
E-mail: adanop@chem.uoa.gr

D. Tzeli
Theoretical and Physical Chemistry Institute
National Hellenic Research Foundation
48 Vassileos Constantinou Ave., 116 35 Athens, Greece

Supporting information for this article is available on the WWW under https://doi.org/10.1002/cphc.202500012

of the N-substituents and/or increase of the N—C^{NHC}—N angle, irrespective of the solvent;.[10] 3) The nucleophilicity of NHCs seems to be largely dependent on both the nature of the backbone and the N-substituents of the molecule;[54] 4) the singlet–triplet (S–T) gap,[21,55,56] corresponding to the energy difference between the triple state (T_1) and ground singlet state (S_0), that is, S–T gap = $E(T_1) - E(S_0)$; this concept can be readily expanded and used for the description of the bonding properties of metal complexes[43,57–60] and materials,[61] and the photophysical properties, thereof,[62,63] all of the above being of particular interest in the field of NHCs. The S–T gap of carbenes (NHCs or not) has been shown, from quite early, that affects generally their bonding interactions and especially their dimerization,[21,55] which is also controlled, by the steric bulk of the N-substituents for NHCs.[64,65] 5) The highest occupied molecular orbital - lowest unoccupied molecular orbital (HOMO–LUMO) (H–L) energy difference, which is regarded as an oversimplification of the S–T gap, based on Koopman's theorem is an important metric. 6) Quantities, such as chemical potential and chemical hardness, that are commonly used as reactivity descriptors are related to the H–L gap.[66]

In addition to the above, additional oversimplifications are encountered in the literature regarding the notion that the NHCs have a σ- and π-symmetry orbital which are assigned to their HOMO and LUMO ones, respectively; this is not always the case as highlighted previously by us[67] and others.[42,44] Regarding the S–T gap, many of the papers cited above have not explicitly stated whether the implied energy gap is a vertical (i.e., the energy difference between the triplet and singlet electronic states, on the singlet geometry), an adiabatic (i.e., the energy difference between the triplet and singlet electronic states, on the respective relaxed geometries), or even if it is indeed appropriate to use the two parameters indiscriminately. Since the S–T gap has been shown to earmark the electronic character or the NHC molecules and by extension the electronic structure of complexes containing such ligands and the diversity and ambiguities listed above, the main objectives of this article are the investigation of H–L gap, the vertical, and adiabatic S–T gaps as molecular descriptors.

Regarding the current status of DFT methodology, due to the continuous development of exchange–correlation functionals, a more standard and communal approach to evaluate the electronic structure of molecules is to be looked for. Moreover, the increasing power of modern computers and software development guarantees an even easier description of molecular systems in years to come. Hence, herein, we have carried out a benchmark study on the electronic structures of NHCs using complete active space self-consistent field (CASSCF), n-electron valence 2nd order perturbation theory (NEVPT2), multireference configuration interaction + singles + doubles (MRCISD), and domain-based local pair natural orbital coupled cluster method with single-, double-, and perturbative triple excitations (DLPNO-CCSD[T]) methodologies, while the DLPNO-CCSD(T) results were extrapolated to a complete basis set (CBS) limit. This benchmark study aims to 1) shed light on the interplay between frontier molecular orbitals, H–L gap, S–T gap, and geometry, 2) study the applicability of DFT functionals, and 3) tune of properties of NHCs.

2. Results and Discussion

2.1. The Prototype NHC Structure

As starting point, the 1,3-dimethylimidazol-2-ylidene was studied as a prototype NHC model structure (see **Figure 1**, where the 6, 7 positions are occupied by CH_3). The dependence of its geometry and energetics on different methodologies was evaluated using a series of DFT and *ab initio* methodologies.

First, **1** was optimized using different DFT methodologies that are commonly used in the literature, ranked based on the John Perdew's "Jacob's ladder":[68,69] that is, BP86[70,71] (which is a generalized gradient approximation (GGA) functional), M06[72] and M06-L[73] (which are *meta*-GGA with and without HF-exchange, respectively), B3LYP[74,75] and PBE0[76] (which are hybrid-GGA), TPSSh[77] (which is a hybrid-*meta*-GGA), CAM-B3LYP[78] (which is a long-range-corrected version of B3LYP), and finally, B2PLYP[79] (which is a double-hybrid functional) in conjunction with the def2-TZVPP basis set. Some key geometric data are shown in **Table 1**, demonstrating that the obtained geometry is only slightly dependent on the functional used. This is not surprising, for such a small and symmetrical molecule computed with DFT methods. As for the electronic structure of **1**, **Table 2** contains information on the molecular orbitals of specific character (σ or π), their 3D representations with the respective σ and π symmetry on the C^{NHC}, and the (H–L) gap, which is a commonly used parameter in literature.

The MO that shows strong σ symmetry character on the C^{NHC}-atom is termed "σ orbital" and the respective of π symmetry "π orbital". The shapes of these do not change at different levels of theory (LOT) as shown in Table S1 (see Supporting Information). Moreover, the shape of the LUMO is also consistent but still not of the expected π symmetry. However, at the optimized triplet geometry, the single occupied molecular orbital (SOMO) indeed has π symmetry. Striking though is the difference in the ordering of the MOs and the relative energy of the HOMO and LUMO, which has been impetuously used throughout the years. Even for this prototype structure, the LUMOs are not the expected vacant "π orbitals" at the C^{NHC}, and this fact is reproduced with many different density functionals. We can see, moreover, that upon perturbing the functionals (via traditional perturbation theory, such as MP2 in B2PLYP, or via the short- and long-range corrections in CAM-B3LYP), the ordering of the MOs and the respective H–L gap changes the most. Remarkable is the variation of the calculated H–L gap, which ranges from 4.46 (PB86) to 9.35 eV (B2PLYP), that is, the gap of B2PLYP is more than double of that of PB86. Consequently, from the above, it is concluded that the DFT H–L gap is strongly dependent on the used functional, and thus, it is a poor electronic structure descriptor.

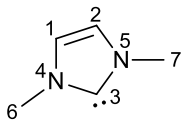

1

Figure 1. Prototype NHC structure, featuring the imidazole backbone and two methyl groups as wingtips.

Table 1. Selected geometries of the prototype **1** obtained using different density functionals and the def2-TZVPP basis set. Distances are given in Å and angles in degrees (°).

Metric	BP86	B3LYP	PBE0	M06-L	M06	TPSSh	CAM-B3LYP	B2PLYP
C1–C2	1.363	1.352	1.350	1.350	1.345	1.354	1.345	1.355
C3–N4, C3–N5	1.373	1.363	1.357	1.364	1.358	1.367	1.355	1.365
C1–N4, C2–N5	1.392	1.386	1.379	1.381	1.382	1.386	1.381	1.384
C6–N4, C7–N5	1.455	1.450	1.441	1.442	1.441	1.452	1.445	1.449
N4-C3-N5	101.76	101.99	102.11	101.53	102.06	101.76	102.44	102.26

Table 2. A series of functionals, with the def2-TZVPP basis set has been used to calculate the H–L gap (in eV) of **1**; given here are the graphical representations of the LUMO and one of the two SOMOs; the latter have been calculated for the optimized geometry of the triplet state, via uDFT. The assignment of the σ and π MOs on the C^{NHC} is also included.

Functional	H–L gap	σ orbital	π orbital	LUMO	SOMO
BP86	4.46	H	L + 1	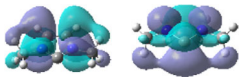	
B3LYP	6.31	H	L + 1	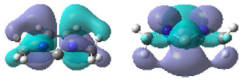	
PBE0	6.81	H	L + 1	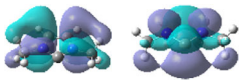	
M06-L	5.05	H	L + 1		
M06	6.76	H	L + 1	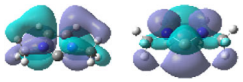	
TPSSh	5.72	H	L + 1	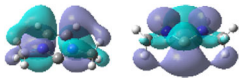	
CAM-B3LYP	9.31	H	L + 3	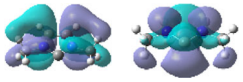	
B2PLYP	9.35	H-1	L + 3	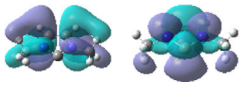	

The above preliminary data showcase that there are limits in the applicability of the various methodologies; while different DFT methodologies led to a divergent H–L gap, all predicting the same geometry. Moreover, we surmise that, absolute values of descriptors, such as the H–L gap, may present issues when different functionals are used, and therefore, systematic studies for families of molecules are needed. In contrast, robust *ab initio* methods are more suitable since they do not feature the many flavors of DFT and are expected to provide a better picture of the electronics of small organic molecules like **1**.

2.2. Derivatives of the Model NHC Structure

Before proceeding with a systematic *ab initio* study, the effect of wingtips of the NHC, which in general has not received much attention, was studied. Analogs of **1** differing in the nature of the wingtips have been studied (**Figure 2**), including more sterically demanding wingtips on the nitrogen atoms; these are more relevant to the community, found in experimental systems.

The geometry of the analogs of **1** has been optimized via DFT (M06-L/def2-TZVPP), both at the lowest in energy singlet and the triplet states, in order to highlight the stark changes in the geometry upon the geometry relaxation of the triplet state (T_1). Consequently, large differences in the geometry between the minimum structures of S_0 and T_1 will result in different relative values of the corresponding vertical and adiabatic S–T gaps. The S_0 and T_1 optimized structures are shown in **Figure 3**. In **Table 3**, the H–L gaps and both the vertical and adiabatic S–T gaps are presented for the molecules of Figure 2, along with those of **1**, as calculated via DFT. Since DFT predicts the geometry well, as a standard for comparison and since, the present system can be handled with *ab initio* methods, DLPNO-CCSD(T)/def2-TZVPP values were also included, which have been performed as single-point (SP) calculations on the DFT-obtained geometries. The assignment of the σ and π MOs on the C^{NHC} atom, the H–L gaps, and the adiabatic and vertical S–T gaps at the M06-L/def2-TZVPP and DLPNO-CCSD(T)/def2-TZVPP methods are given in Table 3. Note that in $\mathbf{1}^{Ph}$, $\mathbf{1}^{Mes}$, and $\mathbf{1}^{DiPP}$, the π symmetry orbital is not strongly localized on the C^{NHC} with strong participation of the aromatic wingtips taking place. Regarding the H–L and S–T gaps within the same DFT methodology, $\mathbf{1}^{Ph}$ presents the smallest

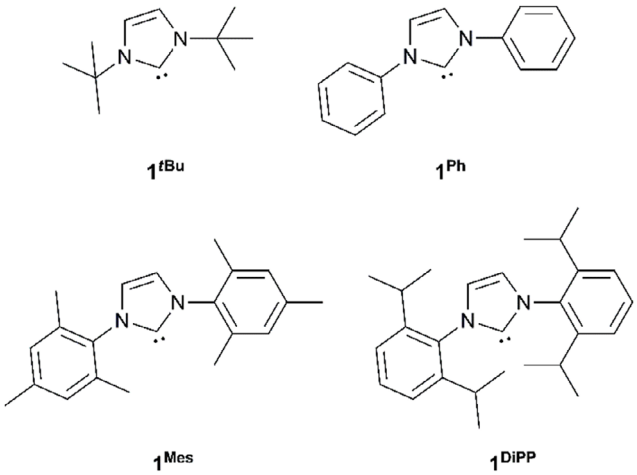

Figure 2. NHC structures derived from **1** by the replacement of the Me wingtips with bulkier tBu, ($\mathbf{1}^{tBu}$); Ph, ($\mathbf{1}^{Ph}$); mesityl (Mes)($\mathbf{1}^{Mes}$); and diisopropylphenyl (DiPP), ($\mathbf{1}^{DiPP}$).

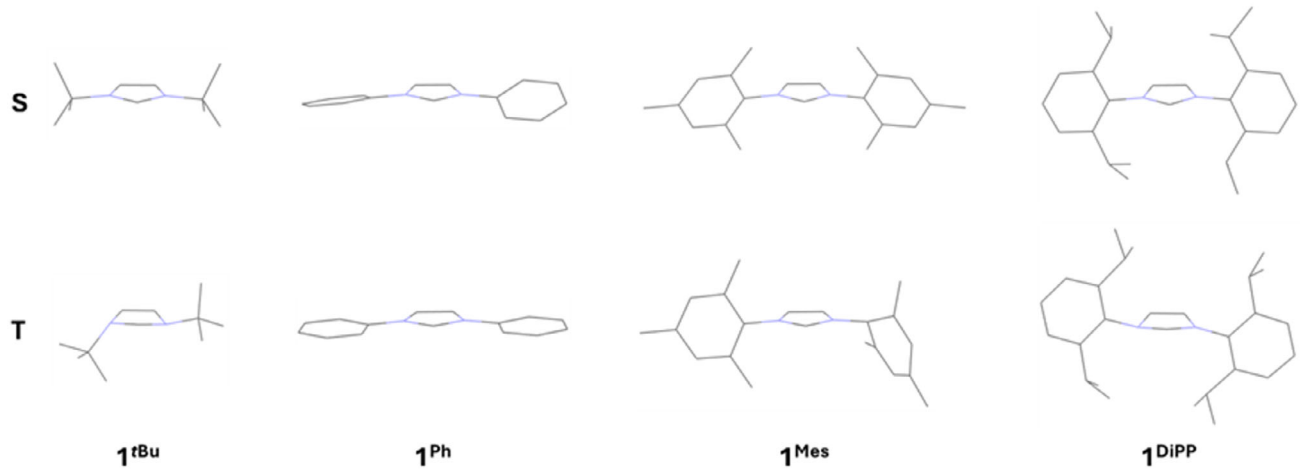

Figure 3. Optimized geometries of analogs of **1**, at the M06-L/def2-TZVPP level of theory. 'S' and 'T' denote the ground singlet and the first excited triplet states, respectively.

Table 3. Assignment of the σ and π MO on the C^{NHC} atom, the H–L gap, and the adiabatic and vertical S–T gaps in eV at the M06-L/def2-TZVPP (DFT) and DLPNO-CCSD(T)/def2-TZVPP (CC) methods.

		1	**1^{tBu}**	**1^{Ph}**	**1^{Mes}**	**1^{DiPP}**
σ orbital		H	H	H	H	H
π orbital		L + 1	L + 1	L	L	L
H–L gap		5.05	5.03	3.86	4.14	4.19
S–T gap (vertical)	CC	5.83	4.50	3.89	4.33	4.34
	DFT	4.26	4.17	3.35	3.90	3.94
S–T gap (adiabatic)	CC	3.91	3.70	3.48	3.48	3.88
	DFT	3.70	3.46	2.92	3.31	3.46

H–L, adiabatic, and vertical S–T gaps, while **1** presents the largest ones. Thus, with the same methodology, there is a consistency for the H–L gap and it can be used as a relative value for comparison.

However, if the H–L gap is used as either an absolute value or as a value that corresponds to the S–T gap, there are some issues encountered. First, the optimized geometry of the triplet state differs substantially from that of the singlet state, thus, leading to a substantially different magnitude between the vertical and adiabatic S–T gaps and ultimately leads to a confusion with respect to which gap is the most appropriate to be used. Second, although useful trends can be extracted from the magnitude of the H–L gap as a substitute (oversimplification) of the S–T gap, this leads to a confusion as for which S–T gap one refers to, and also possible pitfalls may arise, as can be seen, for example, for the case of **1^{Mes}** and **1^{DiPP}**, which have similar values of H–L and vertical S–T gap, but not quite for the relaxed S–T gap. This is also evident when **1** and **1^{tBu}** are compared. Third, the nature of the wingtip also changes the order of the MOs, and for more intricate NHC structures this may lead to even more pronounced changes, and therefore, to problems when one describes the C^{NHC}—M bond in complexes using low-level computational methods. Additionally, the commonly used practice of describing the σ-donating and π-accepting abilities of NHCs through the energies of their frontier MOs also leads to problems. Fourth, the nature of the wingtip also leads to dramatic changes in the (more trustworthy) S–T gap hinting to a problematic situation when one truncates structures to make computational work more manageable. It is not obvious which truncations are benign, as even a methyl group may change both sterics and electronics. Finally, the S–T gap, be it vertical or adiabatic, is a more robust and meaningful way to describe the electronic nature of NHCs, and since, the power and availability of contemporary computers have risen dramatically during the last years, we believe it should be the way to go ahead in the future.

2.3. *N*-Heterocyclic Carbenes and Borylenes

To gain insight in the electronic structure, to compare the vertical and adiabatic S–T gaps, and to check the applicability of the latter as a molecular descriptor, a systematic study was carried out, both via DFT and *ab initio* methods, for the series of NHCs shown in **Figure 4**. Herein, mesoionic NHCs are also included, for which no Lewis structures can be drawn with all-neutral formal charges, and borylenes should serve as a starting point for other main group NHC analogs.

First, optimization calculations were performed for all molecules, using functionals that belong to different levels of "Jacob's ladder", that is, BP86 (GGA), M06-L (*meta*-GGA), B3LYP (hybrid GGA), TPSSh (hybrid *meta*-GGA), and B2PLYP (double-hybrid), both in their singlet and triplet electronic states. As is anticipated for small organic molecules, the differences in the geometries obtained from were insignificant. In contrast to the singlet state, triplet states show considerable geometrical distortion and complete loss of planarity; again, however, the LOT does not affect the geometry much. The energetics, on the other hand, show measurable differences, depending on the LOT being used.

Subsequently, the adiabatic S–T gap was calculated for each functional and ultimately for each molecule; the values are plotted in **Figure 5**. On ascending the "ladder," and therefore the LOT, a remarkably similar trend was observed as to the adiabatic S–T gap. The TPSSh functional yielded the lowest one for all cases, except for the borylene, **9**, for which BP86 gave a slightly lower

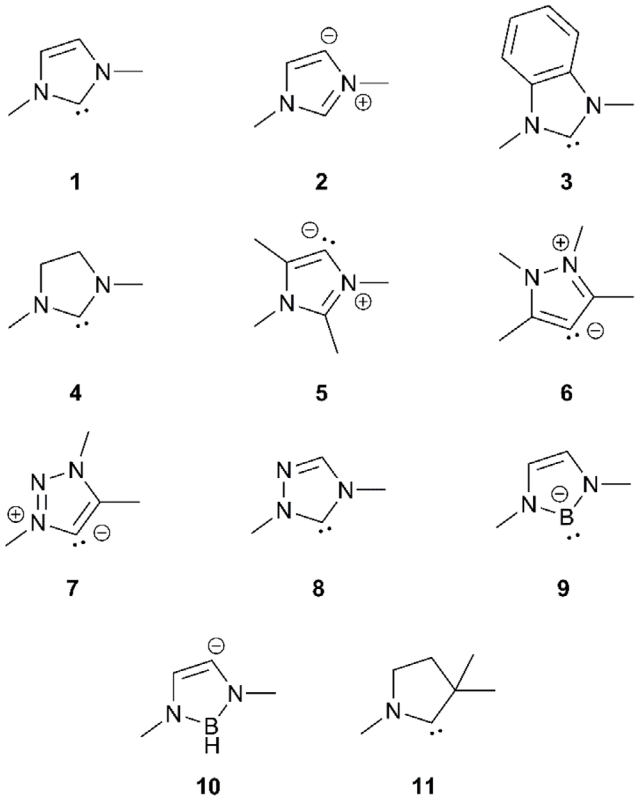

Figure 4. Calculated molecular structures of the *N*-heterocyclic carbenes and borylenes molecules.

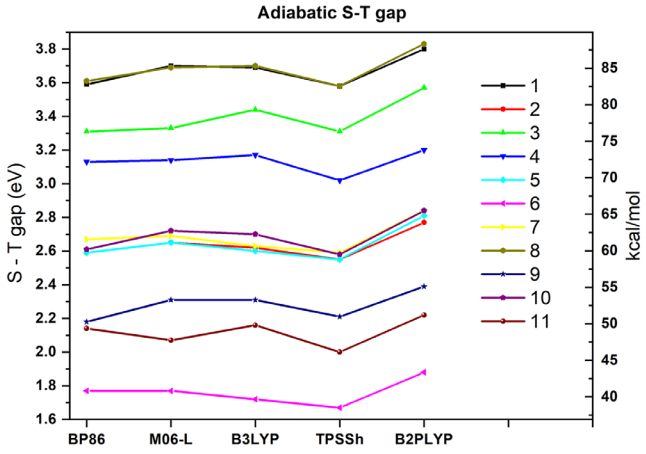

Figure 5. Adiabatic S–T gap for molecules **1**-**11** using a series of DFT methods and the def2-TZVPP basis set. The gap is given both in eV and kcal/mol.

adiabatic S–T gap (50.31 *vs.* 50.97 kcal mol^{-1}). This may be a system-dependent result, since the borylene electronic structure is substantially different, or a functional-dependent result, since BP86 is a GGA functional which, in general, is expected to give lower-level results than a hybrid *meta*-GGA. Analogously, the double-hybrid B2PLYP functional overestimates the adiabatic S–T gap, in all cases, by between 4 and 6 kcal mol^{-1}. In **Table 4**, the average adiabatic S–T gaps are provided, showing that the adiabatic S–T gaps constitute the most consistent DFT

Table 4. Adiabatic S–T gaps (in eV) of molecules **1–11** calculated at the BP86, M06-L, B3LYP, TPSSh, and B2PLYP/def2-TZVPP LOT; the average values are also.

Comp.	BP86	M06-L	B3LYP	TPSSh	B2PLYP	Average[a)]
1	3.59	3.70	3.69	3.58	3.80	3.67
2	2.59	2.65	2.62	2.55	2.77	2.63
3	3.31	3.33	3.44	3.31	3.57	3.39
4	3.13	3.14	3.17	3.02	3.20	3.13
5	2.59	2.65	2.60	2.55	2.81	2.64
6	1.77	1.77	1.72	1.67	1.88	1.76
7	2.67	2.69	2.63	2.59	2.84	2.68
8	3.61	3.69	3.70	3.58	3.83	3.68
9	2.18	2.31	2.31	2.21	2.39	2.28
10	2.61	2.72	2.70	2.58	2.84	2.69
11	2.14	2.07	2.16	2.00	2.22	2.12

[a)]The average deviation is ±0.1 eV.

S–T gap for each molecule, that is, this gap is nearly independent to the used functional.

In Figure 5, the almost equal adiabatic S–T gaps is noticeable in **1** and **8**, despite the latter featuring a third nitrogen atom in the heterocycle, that is, the energy difference between their singlet and triplet states is the same. One could argue that the presence of the additional N-atom in **8** stabilizes both the HOMO and the LUMO, yielding the same H–L gap and ultimately the same S–T gap. The MOs should be used with caution, since, the virtual (empty) orbitals are not optimized in the SCF process and surely have no physical meaning. Indeed, both HOMO and LUMO are lower in energy for **8** compared to **1**, but the stabilization is not of the same magnitude, and the H–L gap is 5.72 and 5.59 eV for **1** and **8**, respectively. These values are obtained at the TPSSh/def2-TZVPP LOT, which features even exactly the same adiabatic S–T gap.

Moreover, compounds **2**, **5**, **7,** and **10**, also feature nearly the same adiabatic S–T gap. Close inspection reveals that they constitute the "abnormal" NHCs, featuring mesoionic structures. In these four molecules, the C^{NHC} atom, showing the carbenic character, is flanked by one N- and one C-atoms; thus, the difference is observed in the backbone, which features different atoms (B, C, N) or groups (H, Me) connected to it. It should be noted that for these molecules the σ-orbital of carbon is the HOMO, as is usually expected, but for B2PLYP, the perturbation makes it HOMO-1 for **5** and **10**.

It seems so far that changes in the "backbone" of the NHC do not produce considerable changes on the adiabatic S–T gap. We can surmise that for structural modifications that do not involve the immediate neighbors of the C^{NHC} atom (i.e., the adjacent atoms), there is no significant change on the adiabatic S–T gap, given that the aromatic character of the heterocycle does not change markedly. Consequently, taking as an example the group of compounds **1**, **3,** and **8**, which share the same N—C^{NHC}—N unit on disparate backbones, in **1** and **8,** we encounter comparable S–T gaps (vide supra); for **3**, however, a lower S–T gap (≈6 kcal mol^{-1}, see Table 4) is calculated which can be ascribed to

the introduction of a fused aromatic ring that interferes with the electronic nature of the molecule.

Moreover, it is worth noting that despite the abovementioned small difference in the adiabatic S–T gap, **1**,**3,** and **8** feature the highest magnitudes of the S–T gaps (also in agreement with results obtained using accurate *ab initio* methods, *vide infra*); this may be ascribed to their aromatic character. Potential aromaticity may be implicated in other molecules of Figure 4 that are, however, either charged or feature charge separation (mesoionic compounds) implying that the charge separation may be an indicator of a lower S–T gap.

Since the adiabatic excitation to the triplet state involves large rearrangement of the geometry of molecules, the "aromatic stabilization" of the molecule will play a decisive role in the final S–T gap. Conversely, the introduction of a nitrogen atom in the 4- or 5-position of the molecule should not change the adiabatic S–T gap and these three molecules should share the same energy value. Thus, two derivates of **3** (**3**^{a} and **3**^{b}) were calculated by the BP86/def2-TZVPP method (see **Figure 6**). It was found that indeed these three molecules share almost the same adiabatic S–T gap energy value, that is, 3.12 (**3**^{a}) and 3.25 eV (**3**^{b}), compared to 3.31 eV (**3**). Again, while the H–L gap can reproduce the trend of the S–T gap (3.09 (**3**^{a}), 3.35 (**3**^{b}), 3.47 (**3**) eV) the relative differences are increased. Energetics derived from electronic states are far more reliable than energetics derived from molecular orbitals.

Following the general treatment with DFT discussed above, ab initio studies were undertaken. Given that all used functionals predict the same geometries for all calculated compounds and the fact that the structures do not have any significant multireference character, *that is,* the main CASSCF coefficient is over 0.90, as our CASSCF(6,5) calculations show in both singlet and triplet states, the compounds could be calculated accurately via a single-reference method. Thus, we concluded that the DFT-obtained geometries were sufficient. Note that the DFT method includes both static and dynamic correlation energies, but without separating the individual contributions and thus, for molecules that can be described by a single-configuration function predict good geometries.[80] Subsequently, SP *ab initio* calculations, that is, MRCISD, NEVPT2, and DLPNO-CCSD(T), were carried out on the DFT-obtained geometries. Regarding the scalable DLPNO−CCSD(T) method, it has been denoted that it can achieve accuracies very close to the canonical CCSD(T).[81]

As a first step, it is useful to inspect the vertical S–T gap by means of CASSCF, NEVPT2, MRCISD, and DLPNO-CCSD(T) methodologies (**Figure 7**). The active space is set to 6 electrons in 5 orbitals, which resembles the aromatic system of the molecules. This is not entirely correct for **3**, which has an extended conjugated system, but for consistency, it was treated in the same way. For these calculations, the geometry obtained via the higher-rung B2PLYP DF is used, in each respective singlet state. The state-averaged SA-CASSCF wavefunction served as a zeroth-order wavefunction for the NEVPT2 calculation. For the MRCISD calculations, two state-specific calculations were performed.

Here, the situation is not as uniform and clearcut as seen previously in Figure 5, and larger energy differences are observed between the same series. Only **3**, **6,** and **8** have their MRCISD values larger than the DLPNO-CCSD(T) ones. We note also that molecules **2**, **5**, **7,** and **10** are following qualitatively the same trend in their S–T gaps, as was the case in Figure 5. However, they do not have the same energy at this point and also molecule **4** features the same trend, while being quite disparate from the other as for its electronic structure. Therefore, usage of the vertical S–T gap may seem inappropriate at this point, to obtain some meaningful insights. In all cases, however, the DFT-obtained S–T gaps are smaller than the corresponding *ab initio* values, see Figure 7.

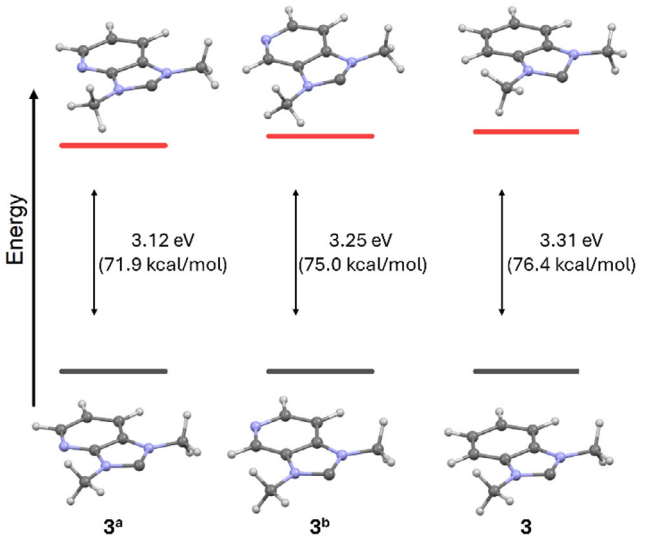

Figure 6. Relative (adiabatic) S–T gaps for **3** (right) and two derivatives (**3a** and **3b**) of it (left, middle). The optimized geometries for all singlet (black lines, down) and triplet (red lines, up) states are also shown, calculated by the BP86/def2-TZVPP method.

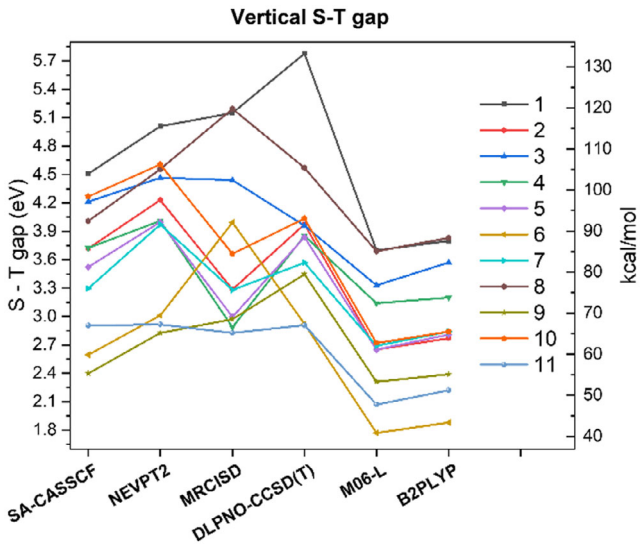

Figure 7. Vertical S–T gap for molecules **1**-**11** calculated via a series of methodologies using the def2-TZVPP basis set. The M06-L geometries have been used for the CASSCF, NEVPT2, MRCISD, and DLPNO-CCSD(T). The respective DFT values from M06-L and B2PLYP are given for comparison purposes.

Since the CASSCF is somewhat restricted and it predicts mainly the static correlation, we expect the MRCISD, NEVPT2, and DLPNO-CCSD(T) methods to retrieve a large amount of dynamical correlation. There are some differences between the MRCISD and DLPNO-CCSD(T) methods. This can be due to several reasons, small active space used in the first, an inherent dubious nature of the vertical S–T gap or issues in DLPNO procedure. Finally, except for **1** and **3**, the NEVPT2 is in better agreement with the DLPNO-CCSD(T) than the MRCISD method. Thus, since there are discrepancies between these three *ab initio* methods, we have proceeded to calculate the adiabatic S–T gap using the MRCI and CC methods. For the sake of completeness, DFT values are also mentioned, where the M06-L values are used, since they are close to the average values and are presented in **Figure 8**.

For all compounds DFT underestimated the adiabatic S–T gap, compared to the DLPNO-CCSD(T) values, and even B2PLYP does so; the latter yielded the biggest S–T gap among the density functionals under study (see Figure 5). For MRCISD + Q, NEVPT2, and DLPNO-CCSD(T), there is no such clear-cut behavior. Strikingly, for almost all the compounds under investigation, the DFT values are closer to the DLPNO-CCSD(T) ones, in comparison with the values obtained via MRCISD or MRCISD + Q. This is not the case for compounds **2**, **6**, **8,** and **11**, however. For **2** and **6**, the DFT and MRCISD values are equidistant to DLPNO-CCSD(T), where in the latter case all three values coincide. For **8** and **11,** the difference is also not that great.

At first sight, this might seem like a "defeat" of the high-level MRCISD and MRCISD + Q methods, but if one considers the importance of the active space, the single- or multireference character of the molecules under study, along with the cancelation of errors of the DFT method, then the DLPNO-CCSD(T) method is bound to yield more significant and reliable results. Indeed, since no bond breaking or forming is happening and the systems do not have a multireference character, the CCSD(T) methods holds firm its title as the "gold standard." Comparing the adiabatic S–T gaps calculated via NEVPT2 with those calculated via MRCISD + Q or DLPNO-CCSD(T), the NEVPT2 values are between the MRCISD + Q and DLPNO-CCSD(T) values. The NEVPT2 values, apart from **3,** are in better agreement with the DLPNO-CCSD(T) values than with the MRCISD + Q adiabatic gaps. Regarding **3**, at the NEVPT2 state, the average CASSCF calculations were carried out resulting in an adiabatic gap of 2.58 eV, while the specific state CASSCF resulted in a value of 4.79 eV. This shows that the active space is not enough for this compound which has a conjugated ring. Thus, for **3,** the DLPNO-CCSD(T) is the best method.

The fact that the M06-L values are very close (≈5 kcal mol^{-1}, except for **3** which is **8** kcal mol^{-1}) to the DLPNO-CCSD(T) values, can be attributed to the cancelation of errors and that the systems under study are small organic molecules. If one goes to use the B2PLYP functional, the energy difference between the DFT and DLPNO-CCSD(T) values is negligible (less than 3 kcal mol^{-1}), which is expected from the best performing level of the molecular density functional theory. It should be noted that DFT contains part of both static and dynamic correlation and the very good agreement between DLPNO-CCSD(T) and DFT is an indication that the adiabatic S–T gap can be regarded as a molecular descriptor.

Quite striking is the large disparity between the MRCISD values with the DFT and DLPNO-CCSD(T) ones, for compounds **4**, **5,** and **7**. For **5** and **7,** this could be attributed to the charge separation, but it is of course not true for **4**.

For completeness, extrapolation to the CBS limit, with the DLPNO-CCSD(T) method, has been performed, using the aug-cc-pV*n*Z, $n = D$, T, and Q basis sets, see **Table 5**. For all compounds, the CBS(3/4) value is given as implemented by ORCA. Apart from **6** and **9,** the extrapolated values are in very good agreement with the DLPNO-CCSD(T)/def2-TZVPP level of theory and the energy difference of the adiabatic S–T gap between DLPNO-CCSD(T)/

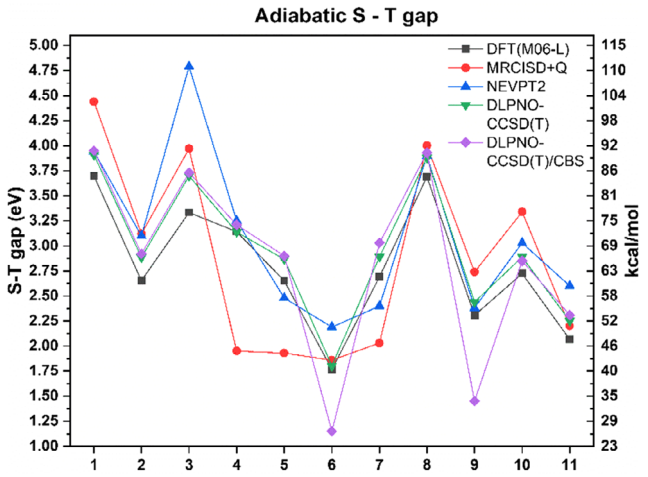

Figure 8. Adiabatic S–T gap for molecules **1**-**11** calculated via DFT (M06-L), MRCISD + Q, NEVPT2, and DLPNO-CCSD(T) (both at def2-TZVPP and CBS) methods, using the M06-L/def2-TZVPP optimized geometries.

Table 5. Benchmark values for the adiabatic S-T gap of the studied **1**-**11** molecules, calculated with the MRCISD,[a] MRCISD + Q,[a] NEVPT2,[a] and DLPNO-CCSD(T) method either by using the def2-TZVPP basis or by extrapolating to the complete basis set using the aug-cc-pVnZ, $n = D$, T and Q basis sets. For all compounds the CBS(3/4) value is given as implemented by ORCA.

Comp.	MRCISD/ def2-TZVPP	MRCISD + Q/ def2-TZVPP	NEVPT2/ def2-TZVPP	DLPNO-CCSD(T)/ def2-TZVPP	DLPNO-CCSD(T)/ CBS
1	4.38	4.44	3.94	3.91	3.95
2	3.11	3.12	3.10	2.88	2.92
3	3.95	3.97	4.79	3.70	3.73
4	1.96	1.95	3.25	3.14	3.21
5	1.96	1.93	2.48	2.87	2.90
6	1.83	1.86	2.19	1.80	1.15
7	2.03	2.03	2.40	2.89	3.03
8	3.99	4.00	3.90	3.88	3.93
9	2.67	2.74	2.38	2.44	1.45
10	3.31	3.34	3.03	2.89	2.85
11	2.21	2.20	2.60	2.25	2.31

[a]State-specific calculations based on CASSCF(6,5).

def2-TZVPP and DLPNO-CCSD(T)/ CBS limit ranges from 0.03 to 0.14 eV. To sum up, it is proposed that a robust and reliable way of calculating the S–T gaps of NHCs is the usage of the DLPNO-CCSD(T) method, while the adiabatic S–T gap can be used as a critical parameter since it is more sensitive to the nature of the NHCs and not so much to the used methodology.

Comparing the adiabatic S–T gap of the calculated compounds obtained with the DLPNO-CCSD(T) method, the NHCs can be arranged with ascending S–T gap as **6** < **11**, **9** < **5**, **2**, **7**, **10** < **4** < **3** < **8** < **1**. Thus, it was found that **1**, **3**, and **8,** which have aromatic character without intense charge separation, present the highest adiabatic S–T gap around 3.9 eV, while **6** which presents intense charge separation has a small gap. It is interesting that the same ordering is retained when the DFT methodology is applied. In other words, the adiabatic S–T gap can be used as a critical molecular descriptor.

2.4. Copper–NHC Complexes

In the light of the previous discussion and to gain insight into the bonding of NHCs and transition metals, we have chosen **1**, **8**, and **11** as model compounds to bind to the "Cu—Cl" moiety, that is frequently encountered in organometallic chemistry,[6] both as a building block of complexes and as a functioning group (**Figure 9**).

The choice of the above NHCs was made on the grounds that **1** and **8** have identical S–T gaps, while **11** has a smaller one and is a privileged ligand in modern organometallic chemistry. Since quite elaborate studies[43] have already been reported on the bonding analysis of such molecules, herein, we only highlight some points relevant to the previous discussion.

First, we have obtained optimized geometries of the three compounds in their singlet and triplet electronic states via DFT (M06-L/def2-TZVPP). SP energies have been calculated with the DLPNO-CCSD(T) method to obtain the vertical and adiabatic S–T gaps. All compounds feature the expected linear C^{NHC}—Cu—Cl geometry at the respective singlet state but undergo pronounced distortion on the (relaxed) triplet state, thus, yielding significant differences between the adiabatic and vertical S–T gaps.

Concerning the geometrical features of the systems, in the singlet state, bond lengths and angles within the NHC moiety change only indiscernibly upon complexation. On the other hand, the relaxed triplet geometry of the NHC ligand features substantial changes compared to the respective complex, indicative of the strong "electronic communication" between the NHC and the metal center. Both the C^{NHC}—Cu and Cu—Cl bonds elongate in the relaxed triplet state for **Cu1** and **Cu8** but remain practically the same for **Cu11**. The change of the C^{NHC}—Cu—Cl angle is also smaller in **Cu11**. This might be an artifact of the present group of complexes or else indicative of the stronger interaction with the CAAC ligand, which has been shown to accommodate triplet states more easily than "normal" NHCs.

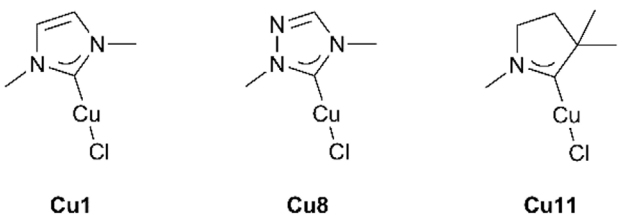

Figure 9. Model calculated compounds featuring the abovementioned NHCs **1**, **8,** and **11**.

The S–T gaps of **Cu1** and **Cu8** follow the same trend as the respective free NHCs, that is, a higher vertical one for **1** and almost identical for the adiabatic ones. For **Cu11**, the two gaps are almost identical (≈2 kcal mol^{-1} difference), which is not the case for **11** (**Figure 10**). The present trend shows that the difference between vertical and adiabatic gaps becomes smaller as the NHC becomes more "electrophilic" or "π-accepting." Therefore, for highly electrophilic NHCs (e.g., those used in photophysics/ photochemistry applications) the use of either one of the two S–T gaps becomes acceptable. Preferring the vertical one is a viable solution due to the lower computational requirements and without losing accuracy. By simple graphical inspection, the spin density of the relaxed complexes on their triplet states is localized on the Cu atom for **Cu1** and **Cu8**, while for **Cu11,** it is localized on the Cu—C^{NHC} bond, consistent with the ability of **11** to stabilize radicals.[49]

Finally, interesting is the fact that the adiabatic S–T gaps between these three compounds are close in energy (≈3.5 kcal mol^{-1}), albeit such a small set of compounds is not able to provide enough statistical certainty as to the interplay between metal and ligand contribution on the S–T gap. The H–L gaps of the M06-L method are 3.80, 3.67, and 2.97 eV. Such values may coarsely capture the general trend or even be close to the actual S–T gap value but their absolute values strongly depend on the used functional.

It is worth mentioning that there are several NHC properties that have also been estimated by quantum chemically which correlate to the S–T gap and reflect the electronic structure and reactivity of NHCs. The quantification of these properties correlates with the relative stability of the singlet or triplet states. Here included are the proton affinity, the dimerization energy, the Tolman electronic parameter (TEP) values, and the electrophilicity at NHC carbon *etc*. 1) The proton affinity (PA) measures the tendency of the NHCs to accept a proton and reflects the basicity of the carbene. Thus, higher PA corresponds to larger S–T gap. 2) Carbenes in a singlet ground state with the lone pair on the carbene carbon are more reactive toward self-dimerization; in contrast, triplet-state carbenes are less likely to dimerize. Therefore, dimerization energy (E_{dim}) may indicate a preference for the singlet or triplet state and be associated with the S–T gap; consequently, large E_{dim} corresponds to large S–T gap.[48] 3) The TEP is derived from IR measurements of carbonyl stretching frequencies in specific metal–carbonyl complexes with NHC ligands.[48] It serves as an indicator of the electronic properties of the NHC in the specific metal–carbonyl complexes and their electron-donating or -withdrawing nature. Stronger electron-donating ligands correspond to lower TEP values and tend to favor the singlet state, resulting in larger S–T energy gaps. 4) Electrophilicity is a measure of the tendency of a molecule to accept electrons. NHCs with low electrophilicity are typically

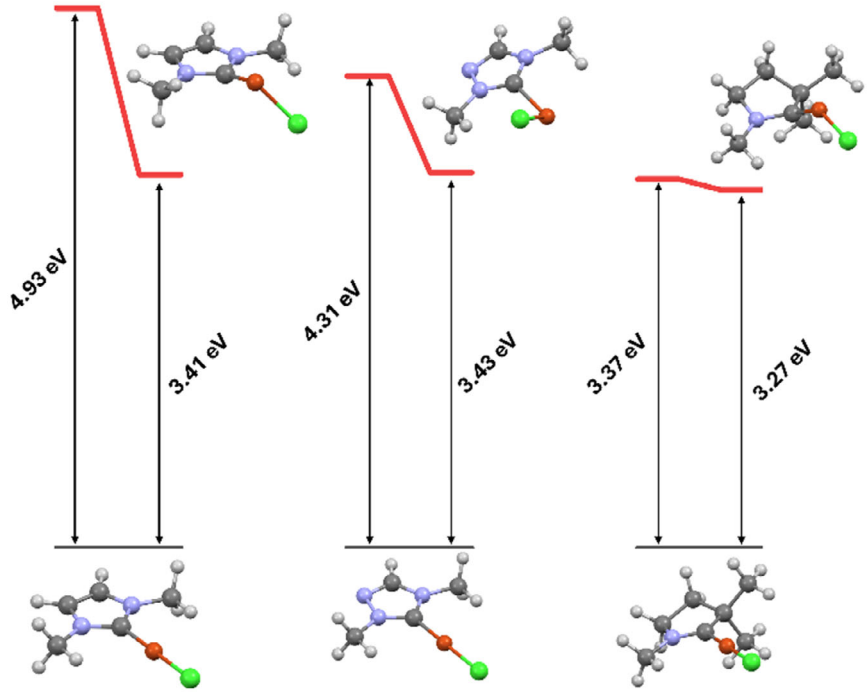

Figure 10. Schematic presentation of the S–T gaps of the model compounds, along with their optimised geometries at the M06-L/def2-TZVPP level of theory. The S–T gaps are obtained via the DLPNO-CCSD(T)/def2-TZVPP. For each complex, the left arrow represents the vertical excitation, while the right one the adiabatic excitation.

better electron donors, and thus, stabilize the singlet state, leading to a large S–T gap. We expect that these parameters should correlate equally well or better with the adiabatic S–T energy gaps than with the vertical S–T energy gaps. Future systematic studies on these properties can elucidate this correlation.

3. Conclusion

Overall, we studied both vertical and adiabatic singlet-triplet gaps of commonly encountered NHCs using a series of DFT methodologies, that is, BP86, M06, M06-L, B3LYP, PBE0, TPSSh, CAM-B3LYP, and B2PLYP, and high-level *ab initio* methods, that is, CASSCF, NEVPT2, MRCISD, and DLNPO-CCSD(T). Finally, the DLNPO-CCSD(T) S–T gaps were extrapolated to the CBS limit.

We found that all DFT methodologies predict the same geometry for a range of NHC molecules, while the absolute value of their calculated HOMO–LUMO gaps is a very much functional dependent quantity. Although DFT is known to provide qualitative trends, this is not always true and the careless use of density functionals may lead to both quantitative and qualitative pitfalls.[82] The excessive use of MO energies and shapes may be even more detrimental to the conclusion reached. For instance, for the 1,3-dimethylimidazol-2-ylidene molecule (**1**), a remarkable variation of the calculated H–L gap is observed, which ranges from 4.46 (PB86) to 9.35 eV (B2PLYP), while the corresponding adiabatic S–T gap ranges from 3.58 (TPSSh) to 3.80 eV (B2PLYP). Thus, energetics derived from electronic states are far more reliable than energetics derived from molecular orbitals.

Based on the results described herein, we suggest the adiabatic S–T gap in general is a more prudent and safer descriptor of NHCs and their complexes than the commonly used H–L gap. The adiabatic S–T gap is more sensitive to the nature and structural features of the NHCs and not so much to the used methodology and thus, fulfills to an extent the requirements for a critical parameter.

Regarding the used high-level *ab initio* methodologies, that is, NEVPT2, MRCISD + Q, and DLNPO-CCSD(T), it is proposed for the NHCs, which do not have a multireference character, the usage of the DLPNO-CCSD(T) method is the best methodology. The combination of the calculation of the geometry via a DFT methodology and the energetics with the DLPNO-CCSD(T) method may lead to very accurate results without the calculations being time consuming.

Regarding the present calculated Cu–NHCs complexes, it was found that their adiabatic S–T gaps follow the same trend as the respective free NHCs, showing that the S–T gaps can be tuned via the selection of the appropriate NHC, which in turn can be calculated separately, thus, diminishing the computational time.

It was found that NHCs having aromatic character without intense charge separation present higher adiabatic S–T gap, while the intense charge separation may lead to a small gap.

Finally, it should be noted that the adiabatic S–T gap can be related to several phenomena. The small the S–T gap may lead to enhanced spin dynamics, that is, enhanced spin-flip transitions, increase intersystem crossings, efficient energy transfer, longer-lived triplet states, and as a result, longer phosphorescence lifetime, while these compounds can play a crucial role in various optoelectronic and photochemical processes.

4. Computational Details

Geometry optimization of all compounds has been performed without any constraints via DFT methods, that is, BP86[70,71] (which is a GGA), M06[72] and M06-L[73] (which are *meta*-GGA with and without HF exchange, respectively), B3LYP[74,75] and PBE0[76] (which are hybrid-GGA), TPSSh[77] (which is a hybrid-*meta*-GGA), CAM-B3LYP[78] (which is a long-range-corrected version of B3LYP), and finally B2PLYP[79] (which is a double-hybrid functional), in conjunction with the def2-TZVPP[83,84] basis set. All DFT calculations were carried out using the Gaussian16[85] package. An ultrafine grid (99 590) was used and during the optimization process the Hessian matrix was explicitly calculated at the beginning and then updated using the Berny algorithm (calcfc command). Points of the potential energy surface with positive-only eigenvalues of the Hessian matrix were deemed as minima.

Single point *ab initio* calculations were performed via the CASSCF, NEVPT2, MRCISD, MRCISD + Q[86] (including the Davidson correction + Q), and DLNPO-CCSD(T)[87] in conjunction with the def2-TZVPP[83,84] basis set at the M06-L/def2-TZVPP obtained geometries. Note that all DFT functionals calculated the same geometries, that is, the differences in distances, angles, and dihedral angles are extremely small (less than 1%). Thus, further optimization via the *ab initio* methods is not carried out.

For the triplet states, a RHF was performed before the CASSCF calculations, while in the DLPNO-CCSD(T) method, at first an unrestricted Hartree–Fock calculation is carried out and then a transformation to quasi-restricted orbitals.

The CASSCF and subsequent MRCISD calculations were carried out using the MOLPRO 2023[88,89] package. The CASSCF and subsequent NEVPT2, as well as the DLNPO-CCSD(T), were obtained using the ORCA4.2.1[90] package.

For both MRCISD and NEVPT2 calculations, a CASSCF calculation served as the zeroth-order wavefunction, with an active space of 6 electrons in 5 molecular orbitals (CASSCF(6,5)) was used. The coefficients of the main reference state configuration, C_0, of the CASSCF and MRCISD calculations are in the range of 0.97–0.98, for all compounds, in either state, supported their single-reference character.

For the CASSCF and subsequent NEVPT2 methods the resolution of identity (RI-JK) approximation was used to speed up the calculation of both Coulomb and Exchange integrals, as implemented in the ORCA4.2.1 package.[91–93]

Finally, extrapolation to a CBS was done using the DLPNO-CCSD(T) method and via the automated code of the ORCA4.2.1 package.[91–93] For this, two-point extrapolations using either aug-cc-pVDZ and aug-cc-pVTZ or aug-cc-pVTZ and aug-cc-pVQZ[94] were used to obtain CBS energies, denoted as CBS(2/3) or CBS(3/4).

Supporting Information

The authors have provided the optimized geometries of all molecules used in this work, in cartesian (*xyz*) coordinates.

Acknowledgements

K.P.Z. acknowledges the Bodossaki Foundation for financial support (M.Sc. scholarship 2023–2024). A.A.D. and D.T. acknowledge support by Special Accounts for Research Grants (S.A.R.G.) of the National and Kapodistrian University of Athens (NKUA). K.P.Z. and D.T. acknowledge computational time granted from the Greek Research & Technology Network (GRNET) in the National HPC facility ARIS under project ID pr015035-TrMeCo.

Conflict of Interest

The authors declare no conflict of interest.

Data Availability Statement

The data that support the findings of this study are available in the supplementary material of this article.

Keywords: *ab initio* · density functional theories · HOMO–LUMO gaps · *N*-heterocyclic carbenes · singlet–triplet gaps

[1] A. Igau, H. Grutzmacher, A. Baceiredo, G. Bertrand, *J. Am. Chem. Soc.* **1988**, *110*, 6463.
[2] A. J. Arduengo, R. L. Harlow, M. Kline, *J. Am. Chem. Soc.* **1991**, *113*, 361.
[3] C. S. J. Cazin, *N-Heterocyclic Carbenes In Transition Metal Catalysis and Organocatalysis*, Springer Netherlands, Dordrecht **2011**.
[4] S. Díez-González, N. Marion, S. P. Nolan, *Chem. Rev.* **2009**, *109*, 3612.
[5] F. Glorius, *N-Heterocyclic Carbenes In Transition Metal Catalysis*, Springer, Berlin, Heidelberg **2007**.
[6] A. A. Danopoulos, T. Simler, P. Braunstein, *Chem. Rev.* **2019**, *119*, 3730.
[7] S. Barik, A. T. Biju, *Chem. Commun.* **2020**, *56*, 15484.
[8] D. M. Flanigan, F. Romanov-Michailidis, N. A. White, T. Rovis, *Chem. Rev.* **2015**, *115*, 9307.
[9] I. Jain, P. Malik, *Eur. Polym. J.* **2021**, *150*, 110412.
[10] M. Fèvre, J. Pinaud, Y. Gnanou, J. Vignolle, D. Taton, *Chem. Soc. Rev.* **2013**, *42*, 2142.
[11] C. A. Smith, M. R. Narouz, P. A. Lummis, I. Singh, A. Nazemi, C. H. Li, C. M. Crudden, *Chem. Rev.* **2019**, *119*, 4986.
[12] Y. Wang, J. P. Chang, R. Xu, S. Bai, D. Wang, G. P. Yang, L. Y. Sun, P. Li, Y. F. Han, *Chem. Soc. Rev.* **2021**, *50*, 13559.
[13] H. Shen, G. Tian, Z. Xu, L. Wang, Q. Wu, Y. Zhang, B. K. Teo, N. Zheng, *Coord. Chem. Rev.* **2022**, *458*, 214425.
[14] C. Cerezo-Navarrete, P. Lara, L. M. Martínez-Prieto, *Catalysts* **2020**, *10*, 1.
[15] A. A. D. Tulloch, A. A. Danopoulos, S. Kleinhenz, M. E. Light, M. B. Hursthouse, G. Eastham, *Organometallics* **2001**, *20*, 2027.
[16] X. Hu, Y. Tang, P. Gantzel, K. Meyer, *Organometallics* **2003**, *22*, 612.
[17] X. Hu, I. Castro-Rodriguez, K. Olsen, K. Meyer, *Organometallics* **2004**, *23*, 755.
[18] D. Nemcsok, K. Wichmann, G. Frenking, *Organometallics* **2004**, *23*, 3640.
[19] H. Jacobsen, A. Correa, C. Costabile, L. Cavallo, *J. Organomet. Chem.* **2006**, *691*, 4350.
[20] D. A. Dixon, A. J. Arduengo, *J. Phys. Chem.* **1991**, *95*, 4180.
[21] C. Heinemann, W. Thiel, *Chem. Phys. Lett.* **1994**, *217*, 11.
[22] M. H. M. Olsson, P. Borowski, B. O. Roos, *Theor. Chim. Acta* **1996**, *93*, 17.
[23] R. R. Sauers, *Tetrahedron Lett.* **1996**, *37*, 149.
[24] G. Raabe, K. Breuer, D. Enders, J. H. Teles, *Z. Naturforsch. A* **1996**, *51*, 95.
[25] C. Boehme, G. Frenking, *J. Am. Chem. Soc.* **1996**, *118*, 2039.
[26] M. Z. Kassaee, F. A. Shakib, M. R. Momeni, M. Ghambarian, S. M. Musavi, *J. Org. Chem.* **2010**, *75*, 2539.
[27] H. V. Huynh, G. Frison, *J. Org. Chem.* **2013**, *78*, 328.
[28] S. K. Schneider, P. Roembke, G. R. Julius, C. Loschen, H. G. Raubenheimer, G. Frenking, W. A. Herrmann, *Eur. J. Inorg. Chem.* **2005**, 2973.
[29] M. M. Hänninen, A. Peuronen, H. M. Tuononen, *Chem. - A Eur. J.* **2009**, *15*, 7287.

[30] M. Der Su, C. C. Chuang, *Theor. Chem. Acc.* **2013**, *132*, 1.
[31] P. Pyykkö, N. Runeberg, *Chem. Asian J.* **2006**, *1*, 623.
[32] P. Pinter, D. Munz, *J. Phys. Chem. A* **2020**, *124*, 10100.
[33] N. Holzmann, A. Stasch, C. Jones, G. Frenking, *Chem. - A Eur. J.* **2011**, *17*, 13517.
[34] I. Fernández, C. A. Dyker, A. DeHope, B. Donnadieu, G. Frenking, G. Bertrand, *J. Am. Chem. Soc.* **2009**, *131*, 11875.
[35] P. Schmid, F. Fantuzzi, J. Klopf, N. B. Schröder, R. D. Dewhurst, H. Braunschweig, V. Engel, B. Engels, *Chem. - A Eur. J.* **2021**, *27*, 5160.
[36] R. Tonner, G. Frenking, *Chem. - A Eur. J.* **2008**, *14*, 3260.
[37] X. F. Zhang, M. J. Sun, Z. X. Cao, *Theor. Chem. Acc.* **2016**, *135*, 1.
[38] B. Chen, A. Y. Rogachev, D. A. Hrovat, R. Hoffmann, W. T. Borden, *J. Am. Chem. Soc.* **2013**, *135*, 13954.
[39] D. G. Gusev, *Organometallics* **2009**, *28*, 6458.
[40] R. Tonner, G. Frenking, *Organometallics* **2009**, *28*, 3901.
[41] J. Mathew, C. H. Suresh, *Inorg. Chem.* **2010**, *49*, 4665.
[42] D. M. Andrada, N. Holzmann, T. Hamadi, G. Frenking, *Beilstein J. Org. Chem.* **2015**, *11*, 2727.
[43] J. C. Bernhammer, G. Frison, H. V. Huynh, *Chem. - A Eur. J.* **2013**, *19*, 12892.
[44] D. Munz, *Organometallics* **2018**, *37*, 275.
[45] A. A. Tukov, A. T. Normand, M. S. Nechaev, *Dalton Trans.* **2009**, 7015.
[46] K. Breitwieser, H. Bahmann, R. Weiss, D. Munz, *Angew. Chem. - Int. Ed.* **2022**, *61*, e202206390.
[47] R. Tonner, G. Heydenrych, G. Frenking, *ChemPhysChem* **2008**, *9*, 1474.
[48] D. J. Nelson, S. P. Nolan, *Chem. Soc. Rev.* **2013**, *42*, 6723.
[49] K. Breitwieser, D. Munz, *Cyclic (Alkyl)(Amino)Carbene (CAAC) Ligands: Electronic Structure and Application as Chemically- and Redox-Non-Innocent Ligands And Chromophores*, Elsevier Inc., Amsterdam **2022**.
[50] B. Maji, M. Breugst, H. Mayr, *Angew. Chem. - Int. Ed.* **2011**, *50*, 6915.
[51] A. M. Magill, K. J. Cavell, B. F. Yates, *J. Am. Chem. Soc.* **2004**, *126*, 8717.
[52] D. Martin, N. Lassauque, B. Donnadieu, G. Bertrand, *Angew. Chem. - Int. Ed.* **2012**, *51*, 6172.
[53] E. M. Higgins, E. M. Higgins, J. Armstrong, R. S. Massey, R. W. Alder, A. M. C. O'Donoghue, *Chem. Commun.* **2011**, *47*, 1559.
[54] A. Levens, F. An, M. Breugst, H. Mayr, D. W. Lupton, *Org. Lett.* **2016**, *18*, 3566.
[55] E. A. Carter, W. A. Goddard, *J. Phys. Chem.* **1986**, *90*, 998.
[56] I. Alkorta, J. Elguero, *Chem. Phys. Lett.* **2018**, *691*, 33.
[57] N. Le Phuoc, A. C. Brannan, A. S. Romanov, M. Linnolahti, *Molecules* **2023**, *28*, 4398.
[58] D. Munz, *Chem. Sci.* **2018**, *9*, 1155.
[59] M. Reiher, *Inorg. Chem.* **2002**, *41*, 6928.
[60] I. Efremenko, E. Poverenov, J. M. L. Martin, D. Milstein, *J. Am. Chem. Soc.* **2010**, *132*, 14886.
[61] G. Han, Y. Yi, *Angew. Chem. - Int. Ed.* **2022**, *61*, 1.
[62] R. Keruckiene, A. A. Vaitusionak, M. I. Hulnik, I. A. Berezianko, D. Gudeika, S. Macionis, M. Mahmoudi, D. Volyniuk, D. Valverde, Y. Olivier, K. L. Woon, S. V. Kostjuk, S. Reineke, J. V. Grazulevicius, G. Sini, *J. Mater. Chem. C Mater.* **2024**, *12*, 3450.
[63] A. Steffen, B. Hupp, *Design of Efficient Emissive Materials*, Elsevier Inc., Amsterdam **2021**.
[64] R. W. Alder, P. R. Allen, M. Murray, A. G. Orpen, *Angew. Chem. Int. Ed* **1996**, *35*, 1121.
[65] M. K. Denk, A. Thadani, K. Hatano, A. J. Lough, *Angew. Chem. Int. Ed Engl.* **1997**, *36*, 2607.
[66] R. A. Miranda-Quintana, *Theor. Chem. Acc.* **2017**, *136*, 1.
[67] F. He, K. P. Zois, D. Tzeli, A. A. Danopoulos, P. Braunstein, *Coord. Chem. Rev.* **2024**, *514*, 215757.
[68] J. P. Perdew, *MRS Bull.* **2013**, *38*, 743.
[69] J. P. Perdew, K. Schmidt, in *AIP Conf. Proc.* Antwerp, Belgium **2001**, Vol. *577*, p. 1.
[70] A. D. Becke, *Phys. Rev. A* **1988**, *38*, 3098.
[71] J. P. Perdew, *Phys. Rev. B* **1986**, *33*, 8822.
[72] Y. Zhao, D. G. Truhlar, *Theor. Chem. Acc.* **2008**, *120*, 215.
[73] Y. Zhao, D. G. Truhlar, *J. Chem. Phys.* **2006**, *125*, 194101.
[74] A. D. Becke, A. D. Becke, *J. Chem. Phys.* **1993**, *98*, 5648.
[75] C. Lee, W. Yang, R. G. Parr, *Phys. Rev. B* **1988**, *37*, 785.
[76] C. Adamo, V. Barone, *J. Chem. Phys.* **1999**, *110*, 6158.
[77] V. N. Staroverov, G. E. Scuseria, J. Tao, J. P. Perdew, *J. Chem. Phys.* **2003**, *119*, 12129.
[78] T. Yanai, D. P. Tew, N. C. Handy, *Chem. Phys. Lett.* **2004**, *393*, 51.
[79] S. Grimme, *J. Chem. Phys.* **2006**, *124*, 034108.
[80] D. Tzeli, P. Golub, J. Brabec, M. Matoušek, K. Pernal, L. Veis, S. Raugei, S. S. Xantheas, *J. Chem. Theory. Comput.* **2024**, *20*, 10406.
[81] Y. Wei, S. Debnath, J. L. Weber, A. Mahajan, D. R. Reichman, R. A. Friesner, *J. Chem. Phys. A* **2024**, *128*, 5796.
[82] K. P. Zois, D. Tzeli, *Atoms* **2024**, *12*, 65.
[83] F. Weigend, *Phys. Chem. Chem. Phys.* **2006**, *8*, 1057.
[84] F. Weigend, R. Ahlrichs, *Phys. Chem. Chem. Phys.* **2005**, *7*, 3297.
[85] Gaussian 16, Revision C.01, M. J. Frisch, G. W. Trucks, H. B. Schlegel, G. E. Scuseria, M. A. Robb, J. R. Cheeseman, G. Scalmani, V. Barone, G. A. Petersson, H. Nakatsuji, X. Li, M. Caricato, A. V. Marenich, J. Bloino, B. G. Janesko, R. Gomperts, B. Mennucci, H. P. Hratchian, J. V. Ortiz, A. F. Izmaylov, J. L. Sonnenberg, D. Williams-Young, F. Ding, F. Lipparini, F. Egidi, J. Goings, B. Peng, A. Petrone, T. Henderson, D. Ranasinghe, et al, Gaussian, Inc., Wallingford CT **2016**.
[86] S. R. Langhoff, E. R. Davidson, *Int J Quantum Chem* **1974**, *8*, 61.
[87] C. Riplinger, F. Neese, *J. Chem. Phys.* **2013**, *138*, 034106.
[88] H. J. Werner, P. J. Knowles, G. Knizia, F. R. Manby, M. Schütz, *Rev. Comput. Mol. Sci.* **2012**, *2*, 242.
[89] H. J. Werner, P. J. Knowles, F. R. Manby, J. A. Black, K. Doll, A. Heßelmann, D. Kats, A. Köhn, T. Korona, D. A. Kreplin, Q. Ma, T. F. Miller, A. Mitrushchenkov, K. A. Peterson, I. Polyak, G. Rauhut, M. Sibaev, *J. Chem. Phys.* **2020**, *152*, 144107.
[90] F. Neese, J. Wiley, *Rev. Comput. Mol. Sci.* **2012**, *2*, 73.
[91] S. Zhong, E. C. Barnes, G. A. Petersson, *J. Chem. Phys.* **2008**, *129*, 184116.
[92] F. Neese, E. F. Valeev, *J. Chem. Theory. Comput.* **2011**, *7*, 33.
[93] T. Helgaker, W. Klopper, H. Koch, J. Noga, *J. Chem. Phys.* **1997**, *106*, 9639.
[94] R. A. Kendall, T. H. Dunning, R. J. Harrison, *J. Chem. Phys* **1992**, *96*, 6796.

Manuscript received: January 14, 2025
Revised manuscript received: March 27, 2025
Version of record online: March 27, 2025